Tetrahedron xxx (2018) 1–8

Contents lists available at ScienceDirect

Tetrahedron

journal homepage: www.elsevier.com/locate/tet

N-(acridin-9-yl)arenesulfonamides: Synthesis, quantum chemical studies and crystal structure analysis to establish the tautomeric preferences

Sumit S. Chourasiya [a], Aabid A. Wani [a], C.M. Nagaraja [b], Asit K. Chakraborti [a, **], Prasad V. Bharatam [a, *]

[a] Department of Medicinal Chemistry, National Institute of Pharmaceutical Education and Research (NIPER), Sector 67, S.A.S. Nagar, 160 062, Punjab, India
[b] Department of Chemistry, Indian Institute of Technology (IIT) Ropar, Roopnagar, 140 001, Punjab, India

ARTICLE INFO

Article history:
Received 26 March 2018
Received in revised form
6 May 2018
Accepted 8 May 2018
Available online xxx

Keywords:
Ring-chain
Isomerism
DFT
Guanylhydrazone
NMR

ABSTRACT

The potentiality of the N-(acridin-9-yl)arenesulfonamide moiety as a hybrid pharmacophore due to the distinct pharmacological activities of acridines and aryl/heteroaryl sulfonamides prompts to synthesise N-(acridin-9-yl)arenesulfonamides and study their structural properties. Various N-(acridin-9-yl)arene/heteroarenesulfonamides were obtained through the development of a new methodology adopting the $Pd_2(dba)_3$-catalyzed C–N bond formation strategy for the reaction of 9-chloloroacridine with arene/heteroarenesulfonamides. The 1H and ^{13}C NMR spectra suggest these N-(acridin-9-yl)arene/heteroarenesulfonamides to exist solely as the sulfonimide tautomer rather than anticipated sulfonamide form and was confirmed by the single crystal XRD analysis of one of the newly synthesized compounds. The quantum chemical studies rationalized this tautomeric preference revealing that the sulfonimide tautomers are more stable than the sulfonamide tautomers by −0.67 to −5.12 kcal/mol in the gas phase. In the solid state, the sulfonimide tautomer is stabilized by intermolecular hydrogen bond between N–H···O–S and π– π stacking between the acridine rings.

1. Introduction

The acridine moiety exerts its anticancer activity by intercalating between base pairs of double-stranded DNA through π-π interactions[1,2] and represents the essential pharmacophoric feature of drugs such as amsacrine (anticancer),[3] mepacrine (antimalarial),[4] proflavin (topical antiseptic, antibacterial)[5] (Fig. 1A). On the other hand, sulfonamides have long been the subject of pharmaceutical interest due to their diverse biological activities[6] and solid state structural properties (originating from polymorphism and tautomerism).[7,8] The sulfonamide group contributes to the pharmacophoric features in many drugs including the recently approved bosentan (antihypertensive),[9] sulfasalazine (antibacterial),[10] sulfadiazine (antibacterial),[11] sulfathiazole (antibacterial),[12] sulfamethoxazole (antibacterial),[13] sulfamethazine[14] (Fig. 1B).

Many hybrid sulfonamides with different heterocycles have gained attention for the development of drugs/leads. The recent examples include (i) chloroquinoxaline sulfonamide (NSC-339004)[15,16] is a synthetic heterocyclic sulfonamide which has been identified as investigational drug for the treatment of cancer, is in the clinical trial stage.

Chloroquinoxaline was tested and found to be both a topoisomerase-IIa and a topoisomerase-IIb poison; (ii) BMS-193884[17] which contain isoxazole sulfonamide moeity was identified as endothelin receptor antagonist, (iii) AM-0466[18] and PF-050897771[19] are clinical candidate with selective sodium channel (Nav1.7) inhibitory activity for the management of pain; (iv) a quinazoline sulfonamide derivative[20] has been reported as anticancer agent. (Fig. 2A). All these examples represent the hybrid sulfonamides with different heterocycles. Considering the importance of these two moieties (acridine and sulfonamide) in medicinal chemistry, *N*-(acridine-9-yl)arenesulfonimide (NAAS) can also

* Corresponding author. Department of Medicinal Chemistry, National Institute of Pharmaceutical Education and Research (NIPER), S. A. S. Nagar, Punjab, 160 062, India.
** Corresponding author.
E-mail addresses: akchakraborti@niper.ac.in (A.K. Chakraborti), pvbharatam@niper.ac.in (P.V. Bharatam).

https://doi.org/10.1016/j.tet.2018.05.024
0040-4020/

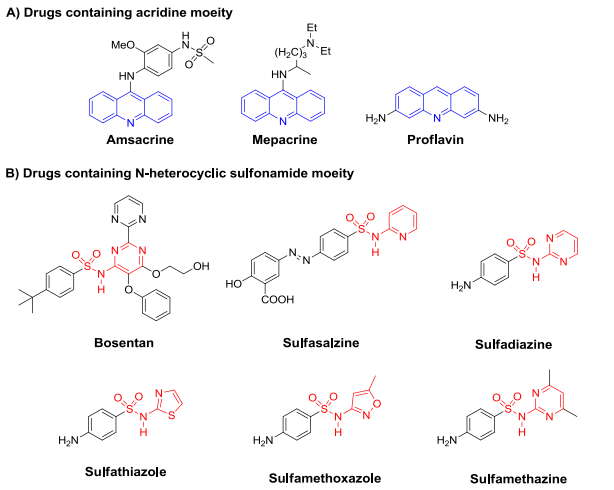

Fig. 1. A) Representative drugs containing the acridine moeity; B) Drugs containing N-heterocyclic sulfonamide moieties.

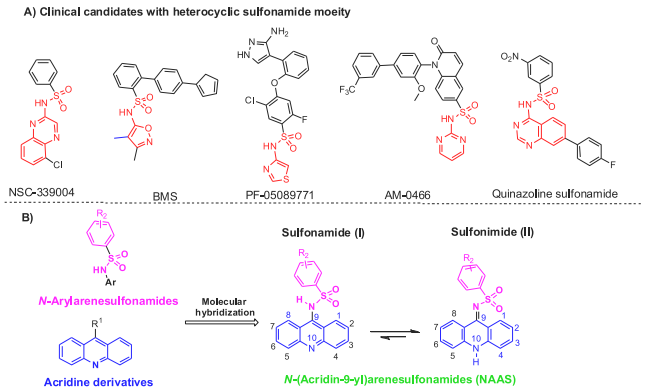

Fig. 2. A) Clinical sulfonamide candidates with different heterocycles; B) NAAS considered in present study representing a hybrid pharmacophore of sulfonamide and acridine moeity. The equilibrium represents the possible sulfonamide-sulfonimide tautomers of NAAS.

be considered as novel hybrid pharmacophore (Fig. 2B).

It is surprising to note that hybrid of sulfonamide and acridine heterocycle as a pharmacophore was not explored till now, the reason could be the non availability of method of its synthesis or difficulty in synthesis of this class of compound. Thus, herein, we report, the synthesis of NAAS through the development of palladium catalyzed method. The quantum chemical studies were carried out to rationalize the formation of sulfonimide tautomer as the sole product, and finally the crystal structure analysis was carried out to confirm the tautomeric preferences.

Tautomerism in drugs is a topic of contemporary interest due to its importance in medicinal chemistry,[21–24] computer-aided drug design,[25–28] drug delivery,[29] drug discovery,[30] understanding the interactions of the drug molecules with the biological targets[31,32] chemical reactivity,[33] structural property[34] and polymorphism.[35] Our lab has been extensively working on the importance of pharmacophoric feature vs tautomer of medicinally important compounds.[23,36–40] Continuing the effort, it was realized that NAAS can represent a pharmacophore and can exhibit tautomeric preference towards sulfonimide tautomer, the results are presented below.

2. Results and discussion

2.1. Synthesis

Due to the lack of information on the synthesis of such class of molecules,[41] initially, we adopted S–N bond formation strategy for the synthesis of *N*-(acridin-9-yl)benzenesulfonamide **3a′** from the reaction of 9-aminoacridine (**1**) and benzenesulfonyl chloride (**2**) using literature reports (Table 1).[42–48] The treatment of 9-aminoacridine (**1**) with benzenesulfonyl chloride (**2**) under various conditions either did not form *N*-(acridin-9-yl)benzenesulfonamide **3a′** (Table 1, entry 1–8) or led to the formation of the bissulfonylated product **4** in poor yield (Table 1, entry 9).

Next, we adopted the C–N bond formation strategy involving the aromatic nucleophilic substitution reaction of 9-chloroacridine (**5**) with arenesulfonamide (**6**) to from *N*-(acridin-9-yl)arenenesulfonamides (**3a′**, Table 2).

The reaction of 9-chloroacridine with arenesulfonamide in the absence of transition metal catalyst gave poor yield of desired product (entry 1–3, Table 2). We observed that the aromatic nucleophilic substitution reaction of heteroarylhalides with arenesulfonamide has been reported under the influence of Cu(I)[49,50] and Pd(II)[51,52] derived catalysts in the presence of suitable ligand and stoichiometric amounts of base but till date there is no report on the reaction of **5** with **6** to form **3′**. Thus, we used the reaction conditions of these literature reports[49–52] for the model reaction of **5** with benzenesulfonamide **6a** so as to find the best operative reaction condition to form **3a′** under the influence of either CuI or $Pd_2(dba)_3$ as the transition metal derived catalysts (TM-Cat) as well as different variation of the reaction conditions such as the use of different ligand, base, and solvent at 80–100 °C (oil bath) for 12 h (Table 2).

The Cu(I)-catalyzed reactions led to either no product formation or produced **3a** in poor yields (GC-MS; ESI) (Table 2, entries 4–10). Amongst the various trials for the $Pd_2(dba)_3$ catalyzed reaction (Table 2, entries 11–16), the best result was obtained in performing the reaction in ^{t}BuOH (Table 2, entry 14) affording **3a** in 56% yield. With this optimized condition in hand, we performed the reaction of **5** with different arenesulfonamides **6** to obtain the *N*-(acridin-9-yl)arenesulfonamides (**3a**-**3o**) in 55–60% yields (Table 3).

Table 1
Synthesis of *N*-(acridin-9-yl)benzenesulfonamide by conventional methods.

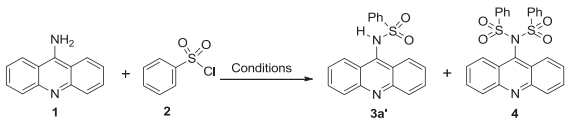

Entry	Reaction conditions	Yield (%)		Literature reports
		3a[a]	**4**	
1	MeCN, Pyridine, rt, 12 h	trace	0	Ref.42
2	Pyridine, 100 °C, 12 h	trace	0	Ref.43
3	H_2O, Na_2CO_3, 80 °C, 12 h	0	trace	Ref.44,4544,4544,45
4	Silica gel, rt, 12 h	0	0	Ref.46
5	EtOH/AcOH, reflux, 12 h	0	0	Ref.47
6	Water, Na_2CO_3, pH = 8, rt, 12 h	0	0	Ref.48
7	MeCN, Na_2CO_3, reflux, 12 h	0	0	Current work
8	MeCN, reflux, 12 h	<5	0	Current work
9	MeCN, K_2CO_3, reflux, 12 h	0	15	Current work

[a] **3a** is the energetically stable sulfonimide tautomer of **3a′** and found to present under experimental condition (*vide infra*).

Please cite this article in press as: Chourasiya SS, et al., N-(acridin-9-yl)arenesulfonamides: Synthesis, quantum chemical studies and crystal structure analysis to establish the tautomeric preferences, Tetrahedron (2018), https://doi.org/10.1016/j.tet.2018.05.024

Table 2
Reaction of **5** with **6a** Under Different Conditions to form **3a′**.

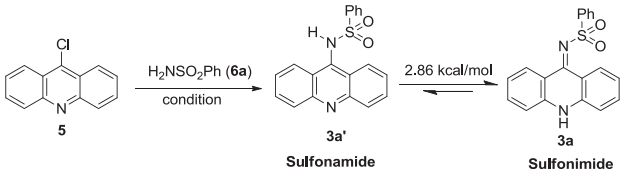

Entry	Catalyst	Ligand	Base	Solvent	Yield (%)[d]
1[a]	**Conc. HCl**	–	–	NMP	0
2[b]	**–**	–	K_2CO_3	DMF	10
3[b]			Et_3N	EtOH	0
4[c]	**CuI**	DMEDA	K_2CO_3	MeCN	<5
5	**CuI**	Glycine	K_2CO_3	^{t}BuOH	0
6	**CuI**	Glycine	K_2CO_3	DMF	15
7	**CuI**	DMEDA	K_2CO_3	dioxane	<5
8	**CuI**	DMEDA	K_2CO_3	PhMe	25
9	**CuI**	DMEDA	K_2CO_3	DMF	27
10	**CuI**	DMEDA	K_2CO_3	^{t}BuOH	<5
11[c]	**$Pd_2(dba)_3$**	Xantphos	Cs_2CO_3	dioxane	15
12	**$Pd_2(dba)_3$**	Xantphos	Cs_2CO_3	PhMe	25
13	**$Pd_2(dba)_3$**	Xantphos	Cs_2CO_3	DMF	28
14	**$Pd_2(dba)_3$**	**Xantphos**	**Cs_2CO_3**	**^{t}BuOH**	**56**
15	**$Pd_2(dba)_3$**	dppf	Cs_2CO_3	^{t}BuOH	42
16	**$Pd_2(dba)_3$**	Xantphos	Cs_2CO_3	MeCN	38

[a] **5** (80 mg, 0.37 mmol) was treated with **6a** in the presence of NMP as solvent (2 mL) with catalytic HCl at rt for 12 h.
[b] **5** (80 mg, 0.37 mmol) was treated with **6a** (1.2 equiv) in the presence of base (3 equiv) in the solvent (2 mL) at 80–100 °C (oil bath) for 12 h.
[c] **5** (80 mg, 0.37 mmol) was treated with **6a** (1.2 equiv) in the presence of the TM-cat **[**CuI (5 mol %); $Pd_2(dba)_3$ (1 mol %)], ligand [DMEDA 0.5, Glycine 0.15, Xantphos/dppf 0.03 equiv], and the base (3 equiv) in the solvent (2 mL) at 80–100 °C (oil bath) for 12 h.
[d] The isolated yield of **3a′**.

2.2. Establishment of tautomeric preferences through NMR spectroscopy

The *N*-(acridin-9-yl)arenesulfonamides can exist either in sulfonamide tautomer and/or sulfonimide tautomer (Scheme 1). The sulfonamide tautomer (**3′**) is characterized by the presence of –NH group exocyclic to the acridine ring whereas sulfonimide tautomer (**3**) is characterized by the exocyclic imine with proton is attached to the endocyclic nitrogen of acridone ring.

To establish the tautomeric preferences, NMR spectroscopic studies on a series of NAAS (**3a-3o**) was carried out. A broad signal at δ 12.7–13.2 was observed in the ^{1}H NMR of the synthesized compounds **3a**-**3o** that appeared to be much downfield in comparison to that of the NH proton (δ 6.84)[53] in *N*-phenylbenzenesulfonamides.

This suggested that **3a**-**3o** exist exclusively in the sulfonimide tautomeric state (**II**, Fig. 2B) as the NH chemical shift values (δ 12.7–13.2 ppm) of **3a**-**3o** are comparable to that of 10-(H)-acridone in which the endocyclic –NH proton appears at δ 11.8 ppm[54,55] Fig. 3 shows a presence of broad singlet at δ 12.88 due to the presence of endocyclic –NH proton in compound **3a** and hence suggest the existence of sulfonimide tautomer.

It was realized that apart from the NH proton chemical shift, the C9 carbon chemical shift values of the sulfonamide and sulfonimide tautomeric forms would be more convincing probe (diagnostic feature) to establish the tautomeric structure of **3a-3o**. In the absence of standard reference, we calculated (GIAO method)[56] the ^{13}C chemical shift values of the C9 carbon of both of the tautomers in each of **3a**-**3o** and observed that the calculated ^{13}C chemical shift values of the C9 carbon in the sulfonimide form compared well with the corresponding experimental values (Table 4). Thus, the compounds **3a**-**3o** exist in the sulfonimide tautomeric state.

Table 3
The $Pd_2(dba)_3$-Catalyzed Reaction of 5 with Various arylsulfonamides (**6**) to Form the N-(acridin-9-yl)arenesulfonamide (**3a-3o**).[a]

Entry	Compd	Ar	Time (h)	Yield (%)[b]
1	**3a**		12	56
2	**3b**	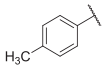	16	57
3	**3c**	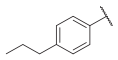	3	3c
4	**3d**		15	60
5	**3e**	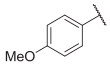	16	55
6	**3f**	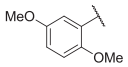	16	59
7	**3g**	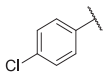	17	50
8	**3h**	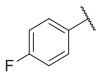	12	55
9	**3i**	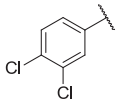	12	54
10	**3j**	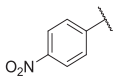	12	55
11	**3k**		16	55
12	**3l**	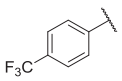	12	56
13	**3m**		14	55
14	**3n**	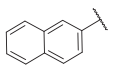	17	57
15	**3o**		13	57

[a] **5** (80 mg, 0.37 mmol) was treated with **6** (1.2 equiv) in the presence of $Pd_2(dba)_3$ (1 mol %), Xantphos (0.03 equiv), and Cs_2CO_3 (3 equiv) in ^{t}BuOH (2 mL) at 80 °C (oil bath) for the indicated time period.
[b] The isolated yield.

2.3. Quantum chemical studies to rationalize the stability of sulfonimide tautomer

We next planned to rationalize the preference of **3a**-**3o** for the sulfonimide tautomer by calculating the tautomeric energy differences (ΔG_T) between the sulfonimide and sulfonamide tautomers

Please cite this article in press as: Chourasiya SS, et al., N-(acridin-9-yl)arenesulfonamides: Synthesis, quantum chemical studies and crystal structure analysis to establish the tautomeric preferences, Tetrahedron (2018), https://doi.org/10.1016/j.tet.2018.05.024

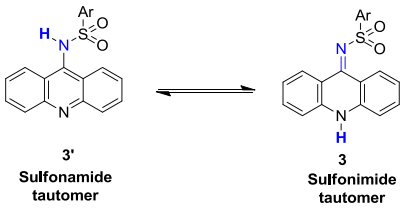

Scheme 1. Two Possible Tautomeric forms (sulfonamide and sulfonimide) of *N*-(acridin-9-yl)arenesulfonamides.

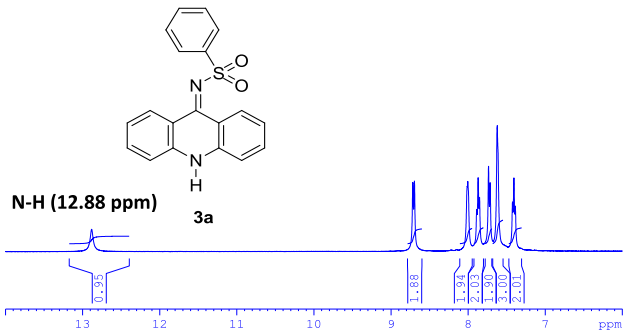

Fig. 3. ^{1}H NMR spectrum of **3a** (N-(acridin-9(10H)-ylidene) benzene sulfonamide) in DMSO-d_6 indicating the presence of sulfonimide tautomer in solution state.

Table 4
Comparison of Experimental and Theoretical δ^{13}C Values (ppm) of C9 for the Sulfonamide and the Sulfonimide Tautomers of **3a-3o** and the ΔG_T (kcal/mol) values.

S. No.	compd	δ^{13}C, C9 (Exp.)	δ^{13}C, C9 (Calc.)		ΔG_T[a]
			Sulfonimide	Sulfonamide	
1	**3a**	159.7	162.9	142.4	−2.86
2	**3b**	160.0	162.8	142.4	−2.19
3	**3c**	160.8	162.5	142.6	−2.21
4	**3d**	159.8	164.8	142.6	−3.74
5	**3e**	159.8	162.9	142.8	−2.07
6	**3f**	160.3	162.9	143.8	−0.81
7	**3g**	160.2	163.2	141.5	−3.84
8	**3h**	160.4	163.1	141.7	−3.38
9	**3i**	160.3	163.1	141.4	−3.96
10	**3j**	160.4	163.7	140.5	−5.12
11	**3k**	160.5	164.2	141.0	−4.32
12	**3l**	160.4	163.3	141.2	−4.24
13	**3m**	159.8	164.6	142.8	−0.67
14	**3n**	160.0	163.2	142.2	−3.27
15	**3o**	163.7	163.6	144.4	−5.14

[a] Sulfonamide ⇋ Sulfonimide tautomeric energy difference, ΔG_T in kcal/mol, where T represent tautomer, calculated at [B3LYP/6-311 + G(d,p) level]. The negative values indicate that sulfonimide tautomer is more stable.

of **3a-3o** (Table 2, col 6) using the density functional B3LYP/6-311 + G(d,p).[57] method to obtain the energy differences (ΔG_T) between the sulfonimide and sulfonamide tautomers (Table 3, col 6). In all cases, the sulfonimide tautomer was found to be more stable than the corresponding sulfonamide form by ~0.67–5.14 kcal/mol. Fig. 4 provides a comparison of the optimized 3D structures of the sulfonamide and sulfonimide tautomers of **3a**. In case of the sulfonamide tautomer, the acridine ring is planar with the C8–C11–C9–C13 torsional angle of 178.8° whereas, in case of the sulfonimide tautomer, the acridine ring adopts a butterfly shape with the C8–C11–C9–C13 torsional angle of 169.8°. The C9–N15 bond lengths were found to be 1.42 Å and 1.30 Å in the sulfonamide and sulfonimide tautomers, respectively. The SO_2 group was found to be out of plane of the acridine ring in the sulfonamide tautomer

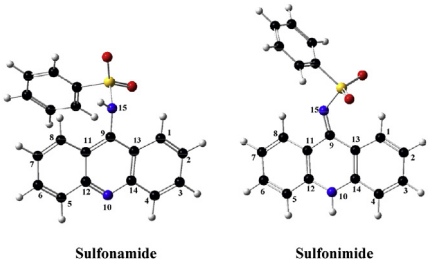

Fig. 4. Quantum chemically [B3LYP/6-311 + G(d,p) level] optimized 3D structures of the sulfonamide and sulfonimide tautomers of **3a** in their monomeric state.

with the C11–C9–N15–S torsional angle of 102.8° whereas, in the sulfonimide tautomer the SO_2 group is almost coplanar with the acridine ring with the C11–C9–N15–S torsional angle of 170.3° (Fig. 4).

The sulfonimide tautomer **3a** shows conjugation of electron density, unlike sulfonamide tautomer which is one of the reasons for the greater stability of sulfonimide tautomer over sulfonamide tautomer. This is clearly evident from the second order delocalization energies of sulfonimide tautomer of **3a** (Table 5). For example, NBO analysis shows that the nN10 → π*C12–C5 second-order delocalization is very strong (~44.27 kcal/mol) in sulfonimide tautomer compared to the sulfonamide tautomer (2.11 kcal/mol). Apart from this interaction, the other second order delocalizations are also important for the stability of sulfonimide tautomer over sulfonamide tautomer which is mentioned in Table 5. This second order delocalization increases the aromaticity of both the benzene rings (A and B, Table 5) of sulfonimide tautomer as compare to the benzene rings of sulfonamide tautomer as it is evident from the nucleus-independent chemical shifts (NICS), a measure of the aromaticity[58–60] which is found to be 8.4 ppm for ring A and ring B in sulfonimide tautomer while it is 8.0 ppm for ring A and 7.1 ppm for ring B of sulfonamide tautomer.

The quantum chemical study suggested that the tautomeric equilibrium is strongly influenced by the polarity of the solvents. For example, the ΔG_T value for **3a** (Ar = Ph) is −2.86 kcal/mol, in gas phase favoring the sulfonimide tautomer. This ΔG_T increases in the order −4.24, −5.68, −5.74, and −5.78 kcal/mol in Et_2O (ε 4.3), MeOH (ε 32.6), DMSO (ε 48.9), and H_2O (ε 78.5), respectively (Table 6)[61,62] suggesting the preference for sulfonimide tautomer increases as the polarity of solvent increases. This is in accordance with the better polar character of the sulfonimide tautomer in comparison to that of the corresponding sulfonamide form (Table S1). These results are in good agreement with our previous

Table 5
NBO Analyses of the Lower Energy Sulfonimide Tautomers of **3a** at B3LYP level using 6-311 + G (d, p) basis set.

Second order delocalization energy E^2 (kcal/mol)		
	Sulfonamide tautomer	Sulfonimide tautomer
	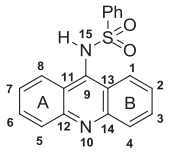	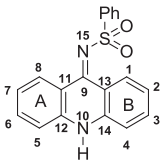
Interactions		
$n_{N10} \rightarrow \pi^*_{C12-C5}$	2.11	44.27
$n_{N15} \rightarrow \pi^*_{C13-C9}$	5.99	8.40
$n_{N15} \rightarrow \pi^*_{C9-C11}$	3.18	11.98
$n_{N15} \rightarrow \pi^*_{C11-C8}$	5.17	1.23

Please cite this article in press as: Chourasiya SS, et al., N-(acridin-9-yl)arenesulfonamides: Synthesis, quantum chemical studies and crystal structure analysis to establish the tautomeric preferences, Tetrahedron (2018), https://doi.org/10.1016/j.tet.2018.05.024

Table 6
Influence of Substituents and Polarity of the Solvents on sulphonamide ⇋ sulfonimide Tautomeric Energy Difference, ΔG_T in kcal/mol, where T represent tautomer, Calculated at B3LYP/6-311++G(d,p) level.

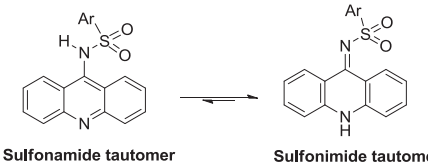

Compd	Substituent (Ar)	ΔG_T (kcal/mol)				
		Gas phase ($\varepsilon = 1$)	Diethyl ether ($\varepsilon = 4.3$)	Methanol ($\varepsilon = 32.7$)	DMSO ($\varepsilon = 46.7$)	Water ($\varepsilon = 80.1$)
3a	Ph	−2.86	−4.24	−5.68	−5.74	−5.78
3b	4-CH_3-Ph	−2.19	−4.81	−5.87	−7.89	−7.83
3c	*n*-Propyl-Ph	−2.21	−4.48	−5.19	−5.34	−5.47
3d	Mesityl	−3.74	−6.03	−6.96	−6.98	−6.98
3e	4-Ome-Ph	−2.07	−4.52	−5.56	−5.64	−5.63
3f	3,4-$(Ome)_2$-Ph	−0.82	−2.29	−2.50	−2.51	−2.55
3g	4-Cl-Ph	−3.84	−5.60	−6.61	−6.66	−6.61
3h	4-F-Ph	−3.38	−5.96	−5.20	−6.73	−6.78
3i	3,4-dichloro-Ph	−3.96	−5.73	−7.72	−6.76	−6.77
3j	4-NO_2-Ph	−5.12	−6.72	−7.35	−7.44	−7.47
3k	3-NO_2-Ph	−4.32	−6.69	−7.27	−6.67	7.12
3l	4-CF_3-Ph	−4.24	−5.81	−7.03	−7.05	−6.77
3m	1-naphthyl	−0.67	−3.29	−4.69	−4.74	−4.79
3n	2-naphthyl	−3.27	−5.07	−5.82	−5.84	−5.79
3o	8-quinolinyl	−5.14	−7.71	−8.49	−9.11	−9.09

studies.[40] However, apart from the polarity (ε) the other physico-chemical parameters of the solvent could also contribute in changing the ΔG_T value with the change in the solvent.[63,64]

The substituents on the aromatic ring were also found to play an important role in dictating the tautomeric equilibrium. In case of **3a** with unsubstituted benzene ring, the ΔG_T in the gas phase is −2.86 kcal/mol (Table 6). The electron withdrawing substituents such as Cl, F, NO_2, CF_3 (**3g**-**3l**) tend to increase the ΔG_T and thus increase the preference towards the sulfonimide tautomer. On the other hand, the electron donating substituents such as Me, ^{n}Pr, and OMe groups (**3b**-**3f**) decrease the ΔG_T (except for compound **3d** in which the two *ortho* Me groups exert steric influence).

2.4. Crystal structure analysis of *3n*

The final proof of concept can be obtained through the crystal structure of some specific examples. We observed that in the only reported crystal structure; **3a** exists in the sulfonimide form.[65]

However, in the absence of detailed crystal structure parameters of this literature report, we planned to obtain the single crystal XRD of the hitherto unknown compound 3n. The single crystal of compound **3n** was obtained from acetonitrile solution by a slow evaporation method. The single crystal was obtained after 15 days and suitable crystals were taken for single crystal XRD analysis.[66] The X-ray structure of **3n** unambiguously confirmed the formation of the compound in its preferred sulfonimide tautomeric state (Fig. 5).

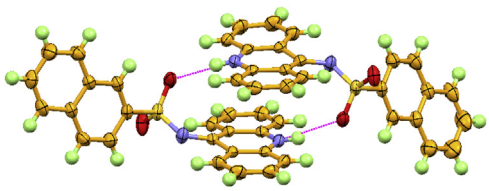

Fig. 5. The ORTEP diagram of **3n** with 50% thermal probability ellipsoids in the dimeric state representing sulfonimide tautomer. (pink dotted lines represent the intermolecular hydrogen bonds).

Quantum chemical analysis was carried out to rationalize the stability of sulfonimide tautomer in its dimeric state. The geometry optimization of sulfonamide dimer and sulfonimide dimer was carried out using B3LYP/ωB97X-D/6-311 + G(d,p) method. The computationally obtained geometrical parameters of the dimer of the sulfonimide tautomer are found to be seamlessly matching with those of the crystal structure (Table 7). The energy difference (ΔG_T) between the dimer of sulfonamide and sulfonimide tautomer was calculated and the results indicate that the sulfonimide dimer is more stable than the sulfonamide dimer by ~16 kcal/mol, also the energy gain due to the dimer formation from the monomer of the sulfonimide tautomer in **3n** is 24.86 kcal/mol in the gas phase (ωB97X-D/6-311 + G(d,p)). Hence it can be concluded that in aggregates these NAAS exist as sulfonimide dimer. The dimerization provides extra stability to the sulfonimide tautomeric state of

Table 7
Important Geometrical Parameters of **3n** Obtained from XRD Analysis. Comparison Between the XRD Data and DFT (B3LYP/ωB97X-D/6-311 + G(d,p)) Data is listed. Distances are in Å and angle is in degree (°).

Parameters	Sulfonimide dimer (3n)[a]		
	Single crystal XRD	DFT	
		B3LYP	ωB97X-D[b]
Bond lengths			
C9—N15	1.329	1.321	1.315
N10—C14	1.360	1.368	1.360
Intermolecular hydrogen bond			
N(10)-H·····O—S	2.115	1.88	1.80
Dihedral angle			
C8—C11—C9—C13	167.80	166.80	167.67

[a] For the ease of calculation and to reduce computational time, the naphthalene ring in compound **3n** was replaced with methyl group.

[b] It is known that the DFT B3LYP functional cannot adequately account for the dispersion interaction[67,68] such as π−π stacking and hence the dispersion corrected DFT functional i.e. ωB97X-D[69] was used.

Please cite this article in press as: Chourasiya SS, et al., N-(acridin-9-yl)arenesulfonamides: Synthesis, quantum chemical studies and crystal structure analysis to establish the tautomeric preferences, Tetrahedron (2018), https://doi.org/10.1016/j.tet.2018.05.024

NAAS.

Next, a comparison of the 3-D optimized structure of sulfonamide dimer and sulfonimide dimer was carried out (Fig. 6). The 3-D optimized structure of sulfonimide dimer indicates that it is stabilized by π-π stacking between two acridine rings and two hydrogen bond interactions between NH⋯O=S (Fig. 6A). However, such dimeric state is not possible in case of sulfonamide tautomer. Many attempts were tried to obtained dimer of sulfonamide tautomer with π-π stacking between two acridine rings, but all attempts lead to sulfonamide dimer with different geometry which is characterized by one N–H⋯N- hydrogen bond interaction and the π-π stacking between the only one phenyl ring of acridine heterocycle (Fig. 6B). Hence, in the crystal structure, the sulfonimide dimer is preferred due to extra stabilization from π-π stacking between two acridine rings and one extra hydrogen bond interaction.

3. Conclusions

The present work reveals for the first time the synthesis of *N*-(acridin-9-yl)arenesulfonamide as a promising pharmacophore using palladium catalysis and sulfonamide-sulfonimide tautomerism therein. The ^{1}H and ^{13}C NMR chemical shift values of the NH proton(s) and the C9 carbon revealed that various substituted *N*-(acridin-9-yl)arenesulfonamides, obtained through the development of a new methodology of Pd(II)-catalyzed reaction of 9-chloroacridine with various arenesulfonamides, predominantly exist as the sulfonimide tautomer that receives confirmatory evidence in the single crystal XRD. The origin of the preference towards the sulfonimide tautomer in the solid state is the intermolecular hydrogen bonds in the dimeric form in the unit cell and the π-π stacking interaction involving the acridine rings and in the solution state due to the more polar character.

4. Experimental section

4.1. Computational methods

The quantum chemical calculations were carried out using GAUSSIAN09[70] suite of programmes. Full geometry optimizations were carried out using DFT[57] calculations using B3LYP[71]/ωB97XD[68] method. The basis set used was 6-311 + G(d,p). Frequency calculations were carried out on all the structures to verify stationary point with zero negative frequency. Implicit solvent study was performed using B3LYP/6-311 + G(d,p) and IEFPCM solvent model.[72] To understand the delocalization of the electron density from the occupied (donor) NBOs to properly unoccupied (acceptor) NBOs within the sulfonamide and sulfonimide tautomer, natural bond orbitals (NBO) analysis[73] was used. Using NBO analysis, the second order delocalization energy was calculated. The ^{13}C NMR chemical shift were estimated using the GIAO method[57] for both the sulfonamide and the sulfonamide tautomers of NAAS **3a-3o**. NICS aromaticity indexes[58–60] (in ppm) at the ring centers (A and B) for sulfonimide and sulfonamide tautomers of NAAS was calculated at the GIAO/B3LYP/6-311 + G (d,p) level. Gibbs free energy difference between the two tautomers (ΔG_T) was considered in all the observations discussed in this article.

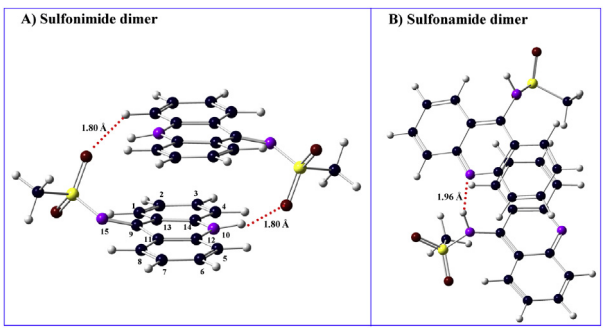

Fig. 6. A) 3D structure of sulfonimide dimer; B) 3D structure of sulfonamide dimer of **3n** obtained from DFT study (ωB97X-D/6-311 + G(d,p)). The red dotted lines indicate the intermolecular hydrogen bonds.

4.2. Chemistry

The reagents and chemicals required for the study were procured from the commercial suppliers and were used as such without further purification. The progress of the reaction was monitored by Thin Layer Chromatography (TLC) performed on silica gel aluminium plates. The visualization of TLC was done by UV light. The ^{1}H NMR and ^{13}C NMR spectra were recorded at 400 MHz and 100 MHz spectrometer respectively, using TMS as an internal standard. The ^{1}H NMR and ^{13}C NMR spectra were recorded for DMSO-d_6 at 2.50 ppm and 39.51 ppm respectively. Chemical shift (δ) are reported in part per million (ppm). Coupling constants (J) were reported in hertz (Hz). The abbreviations used to characterize the signals are as follows: s = singlet, m = multiplet, d = doublet, br s = broad singlet, t = triplet. High resolution mass spectra were taken using ESI-TOF method. Mass spectra were recorded using ESI mode. Melting points were determined by using melting point apparatus.

4.3. General synthesis of N-(acridin-9-yl)-N-(phenylsulfonyl) benzenesulfonamide (4) using conventional method

9-Aminoacridine (100 mg, 0.5 mmol) was added in three portions to the warmed solution of potassium carbonate (211 mg, 1.53 mmol) in 2 mL of MeCN, 108 mg (0.61 mmol) of benzenesulfonyl chloride was added to the solution in 5 portions over a period of 20 min. The reaction mixture was warmed at 60–70 °C for additional 0.5 h, and raised to 80 °C. The reaction mixture was filtered and filtrate was acidified with dilute HCl. The precipitate observed was collected by filtration and washed with water. The crude product **4** was recrystallized with EtOH/Hex (10%) to afford yellow crystal, yield 15.0%. Yellow solid (44 mg, 25%). mp: 220–222 °C; IR (KBr, cm^{-1}): 2924, 1376, 1173, 1084; ^{1}H NMR (400 MHz, DMSO-d_6) δ = 8.26 (d, J = 8.5 Hz, 2H), 8.01–7.84 (m, 8H), 7.75–7.62 (m, 4H), 7.46–7.40 (m, 4H); ^{13}C NMR (100 MHz, DMSO-d_6) δ = 149.9, 137.9, 136.4, 136.0, 131.2, 130.2, 129.9, 129.5, 127.8, 126.0, 124.4; LC-MS (ESI) *m/z*: [M+Na]$^{+}$ Calcd for $C_{25}H_{18}N_2NaO_4S_2$ 497.0606; Found 497.05.

4.4. General synthesis of 3a-3o using palladium catalysis

A dry round bottom flask was cooled to rt under nitrogen, and was charged with $Pd_2(dba)_3$ (3.38 mg, 0.0037 mmol), cesium carbonate (361 mg, 1.11 mmol), and arenesulfonamide (69 mg, 0.44 mmol). Tertiary-butanol (2 mL) was added, followed by ligand, xantphos (6.4 mg, 0.011 mmol) and 9-chloroacridine (80 mg, 0.37 mmol). The resulting suspension was stirred at rt for 5 min, then heated to 80 °C for 12–17 h. The reaction mixture was then cooled to rt and filtered through suction filtration. The organic fraction was evaporated, and the resulting residue was purified by silica gel chromatography with a hexane/Et-OAc as eluent (60:40).

4.4.1. N-(acridin-9(10H)-ylidene)benzenesulfonamide (*3a*)

Orange solid (69 mg, 60%). mp: 256–258 °C; IR (KBr, cm^{-1}): 2925, 1668, 1088, 805; ^{1}H NMR (400 MHz, DMSO-d_6) δ = 12.88 (br s,

Please cite this article in press as: Chourasiya SS, et al., N-(acridin-9-yl)arenesulfonamides: Synthesis, quantum chemical studies and crystal structure analysis to establish the tautomeric preferences, Tetrahedron (2018), https://doi.org/10.1016/j.tet.2018.05.024

1H), 8.71 (d, $J = 8.5$ Hz, 2H), 8.10–7.95 (m, 2H), 7.87 (t, $J = 7.4$ Hz, 2H), 7.73 (d, $J = 8.3$ Hz, 2H), 7.60–7.64 (m, 3H), 7.41 (t, $J = 7.5$ Hz, 2H); ^{13}C NMR (100 MHz, DMSO-d_6) $\delta = 159.7$, 146.0, 140.4, 134.8, 131.7, 129.3, 128.9, 125.8, 122.8, 118.6, 118.2. HRMS (ESI-TOF) *m/z*: $[M+Na]^+$ Calcd for $C_{19}H_{14}N_2O_2SNa$: 357.0668 $[M+Na]^+$; Found 357.0656.

4.4.2. N-(acridin-9(10H)-ylidene)-4-methylbenzenesulfonamide (**3b**)

Yellowish solid (46 mg, 57%). mp: 240–242 °C; IR (KBr, cm^{-1}): 2923, 1630, 1072, 794; ^{1}H NMR (400 MHz, DMSO-d_6) $\delta = 12.84$ (br s, 1 H), 8.70 (d, $J = 8.3$ Hz, 2 H), 7.93–7.81 (m, 4 H), 7.71 (d, $J = 8.3$ Hz, 2 H), 7.45–7.35 (m, 4 H), 2.42 (s, 3 H); ^{13}C NMR (100 MHz, DMSO-d_6) $\delta = 160.0$, 143.3, 141.7, 140.4, 134.8, 129.7, 129.0, 125.9, 122.7, 118.6, 118.2, 21.4; HRMS (ESI-TOF) *m/z*: $[M+Na]^+$ Calcd for $C_{20}H_{16}N_2NaO_2S$: 371.0824 $[M+Na]^+$; Found 371.0793.

4.4.3. N-(acridin-9(10H)-ylidene)-4-propylbenzenesulfonamide (**3c**)

Yellow solid (30 mg, 35%). mp: 246–248 °C; IR (KBr, cm^{-1}): 3278, 2924, 1712, 1075, 818. ^{1}H NMR (400 MHz, DMSO-d_6) $\delta = 12.86$ (br s, 1H), 8.71 (d, $J = 7.3$ Hz, 2H), 7.97–7.81 (m, 4H), 7.78–7.66 (m, 2H), 7.35–7.47 (m, 4H), 2.67 (t., $J = 7.3$ Hz, 2H), 1.65 (sep., $J = 7.3$ Hz, 2H), 0.92 (t, $J = 7.3$ Hz, 3H); ^{13}C NMR (100 MHz, DMSO-d_6) $\delta = 160.8$, 157.7, 140.7, 134.8, 129.8, 128.9, 125.9, 122.7, 118.6, 118.1, 32.5, 24.3, 14.1; HRMS (ESI-TOF) *m/z*: $[M+Na]^+$ Calcd for $C_{22}H_{20}N_2O_2SNa$: 399.1137 $[M+Na]^+$; Found 399.1138.

4.4.4. N-(acridin-9(10H)-ylidene)-2,4,6-trimethylbenzenesulfonamide (**3d**)

Yellow solid (52 mg, 60%). mp: 255–257 °C; IR (KBr, cm^{-1}): 2924, 1712, 1630, 1106, 807; ^{1}H NMR (400 MHz, DMSO-d_6) $\delta = 12.75$ (br s, 1 H), 8.63 (d, $J = 8.3$ Hz, 2H), 7.84 (t, $J = 6.4$ Hz, 2H), 7.69 (d, $J = 8.0$ Hz, 2H), 7.35 (t, $J = 7.7$ Hz, 2H), 7.03 (s, 2H), 2.29 (s, 3H), 2.56 (s, 6 H); ^{13}C NMR (100 MHz, DMSO-d_6) $\delta = 140.4$, 140.0, 137.1, 134.6, 131.7, 129.1, 122.6, 118.7, 118.1, 109.6, 108.9, 22.7, 20.9; HRMS (ESI-TOF) *m/z*: $[M+Na]^+$ Calcd for $C_{22}H_{20}N_2O_2SNa$: 399.1137 $[M+Na]^+$; Found 399.1138.

4.4.5. N-(acridin-9(10H)-ylidene)-4-methoxybenzenesulfonamide (**3e**)

Yellowish solid (62 mg, 55%). mp: 211–213 °C; IR (KBr, cm^{-1}): 2923, 1631, 1074, 828; ^{1}H NMR (400 MHz, DMSO-d_6) $\delta = 12.81$ (br s, 1H), 8.71 (d, $J = 8.0$ Hz, 2H), 7.93 (d, $J = 8.5$ Hz, 2H), 7.86 (t, $J = 7.7$ Hz, 2 H), 7.71 (d, $J = 8.3$ Hz, 2H), 7.39 (t, $J = 7.7$ Hz, 2H), 7.13 (d, $J = 8.8$ Hz, 2H), 3.86 (s, 3H); ^{13}C NMR (100 MHz, DMSO-d_6) $\delta = 161.7$, 159.9, 140.4, 138.2, 134.7, 129.0, 127.9, 122.7, 118.6, 118.1, 114.4, 56.0; HRMS (ESI-TOF) *m/z*: $[M+Na]^+$ Calcd for $C_{20}H_{16}N_2NaO_3S$: 387.0773 $[M+Na]^+$; Found 387.0772.

4.4.6. N-(acridin-9(10H)-ylidene)-2,5-dimethoxybenzenesulfonamide (**3f**)

Greenish solid (54 mg, 59%). mp: 223–225 °C; IR (KBr, cm^{-1}): 3436, 2923, 1630, 1057, 752; ^{1}H NMR (400 MHz, DMSO-d_6) $\delta = 12.80$ (br s, 1H), 8.64 (d, $J = 8$ Hz, 2H), 7.85 (t, $J = 8$ Hz, 2H), 7.71 (d, $J = 8.3$ Hz, 2H), 7.49 (s, 1H), 7.38 (t, $J = 7.4$ Hz, 2H), 7.18–7.13 (m, 2H), 3.78 (s, 3H), 3.66 (s, 3 H); ^{13}C NMR (100 MHz, DMSO-d_6) $\delta = 160.3$, 152.5, 150.9, 140.4, 134.7, 133.9, 129.2, 122.5, 118.9, 118.4, 118.0, 114.9, 113.3, 56.8, 56.2; HRMS (ESI-TOF) *m/z*: $[M+Na]^+$ Calcd for $C_{21}H_{18}N_2NaO_4S$: 417.0879 $[M+Na]^+$; Found 417.0872.

4.4.7. N-(acridin-9(10H)-ylidene)-4-chlorobenzenesulfonamide (**3g**)

Dark yellow solid (43 mg, 50%). mp: 218–220 °C; IR (KBr, cm^{-1}): 3473, 2922, 1632, 1076, 813; ^{1}H NMR (400 MHz, DMSO-d_6) $\delta = 13.01$ (br s, H), 8.68 (d, $J = 8.5$ Hz, 2H), 8.01 (d, $J = 8.5$ Hz, 2H), 7.94–7.84 (m, 2H), 7.74 (d, $J = 8.5$ Hz, 2H), 7.68 (d, $J = 8.5$ Hz, 2H), 7.43 (t, $J = 7.7$ Hz, 2H); ^{13}C NMR (100 MHz, DMSO-d_6) $\delta = 160.2$, 144.9, 140.4, 136.4, 135.0, 129.5, 128.9, 127.9, 123.0, 118.6, 118.3; HRMS (ESI-TOF) *m/z*: $[M+Na]^+$ Calcd for $C_{19}H_{13}ClN_2NaO_2S$: 391.0278 $[M+Na]^+$; Found 391.0277.

4.4.8. N-(acridin-9(10H)-ylidene)-4-fluorobenzenesulfonamide (**3h**)

Yellowish solid (45 mg, 55%). mp: 220–222 °C; IR (KBr, cm^{-1}): 2925, 1631, 1081, 805: ^{1}H NMR (400 MHz, DMSO-d_6) $\delta = 12.98$ (br s, 1H), 8.69 (d, $J = 8.5$ Hz, 2H), 8.07–8.04 (m, 2H), 7.87 (t, $J = 8.5$ Hz, 2H), 7.74 (d, $J = 8.3$ Hz, 2H), 7.51–7.32 (m, 4H); ^{13}C NMR (100 MHz, DMSO-d_6) $\delta = 163.3$ (d, 1JC-F = 248 Hz), 159.6, 142.0 (d, 4JC-F = 3 Hz), 140.0, 134.4, 128.4, 128.2 (d, 3JC-F = 9 Hz), 122.4, 118.1, 117.9, 115.8 (d, 2JC-F = 23 Hz); HRMS (ESI-TOF) *m/z*: $[M+Na]^+$ Calcd for $C_{19}H_{13}FN_2O_2SNa$: 375.0573 $[M+Na]^+$; Found 375.0571.

4.4.9. N-(acridin-9(10H)-ylidene)-3,4-dichlorobenzenesulfonamide (**3i**)

Yellowish solid 51 mg, 54%). mp: 229–231 °C; IR (KBr, cm^{-1}): 3280, 2923, 1630, 1097, 752: ^{1}H NMR (400 MHz, DMSO-d_6) $\delta = 13.14$ (br s, 1 H), 8.65 (d, $J = 8.3$ Hz, 2H), 8.13 (d, $J = 4$ Hz, 1H), 8.01–7.84 (m, 3H), 7.77 (d, $J = 8.5$ Hz, 3H), 7.45 (t, $J = 7.5$ Hz, 2H); ^{13}C NMR (100 MHz, DMSO-d_6) $\delta = 160.4$, 146.4, 140.4, 135.1, 134.6, 132.1, 131.9, 128.7, 127.6, 126.3, 123.2, 118.6, 118.4; HRMS (ESI-TOF) *m/z*: $[M+Na]^+$ Calcd for $C_{19}H_{12}C_{l2}N_2O_2SNa$: 424.9888 $[M+Na]^+$; Found 424.9889.

4.4.10. N-(acridin-9(10H)-ylidene)-4-nitrobenzenesulfonamide (**3j**)

Yellowish solid (49 mg, 55%). mp: 252–254 °C; IR (KBr, cm^{-1}): 2925, 1631, 1081, 805; ^{1}H NMR (400 MHz, DMSO-d_6) $\delta = 13.15$ (br s, 1H), 8.66 (d, $J = 8.0$ Hz, 2H), 8.44 (d, $J = 8.5$ Hz, 2H), 8.25 (d, $J = 8.3$ Hz, 2H), 7.96–7.85 (m, 2H), 7.78 (d, $J = 8.3$ Hz, 2H), 7.45 (t, $J = 7.7$ Hz, 2H); ^{13}C NMR (100 MHz, DMSO-d_6) $\delta = 160.4$, 151.4, 149.2, 140.6, 135.1, 128.7, 127.4, 124.9, 123.2, 118.7, 118.6; HRMS (ESI-TOF) *m/z*: $[M+Na]^+$ Calcd for $C_{19}H_{13}N_3O_4SNa$: 402.0518 $[M+Na]^+$; Found 402.0518.

4.4.11. N-(acridin-9(10H)-ylidene)-3-nitrobenzenesulfonamide (**3k**)

Yellow solid (49 mg, 55%). mp: 250–252 °C; IR (KBr, cm^{-1}); 2935, 1641, 1061, 815; ^{1}H NMR (400 MHz, DMSO-d_6) $\delta = 13.20$ (br s, 1H), 8.68–8.64 (m, 2H), 8.44 (d, $J = 8.0$ Hz, 2H), 8.47 (d, $J = 6.5$ Hz, 2 H), 7.98–7.87 (m, 2H), 7.79 (d, $J = 8.3$ Hz, 2H), 7.45 (t, $J = 7.4$ Hz, 2 H); ^{13}C NMR (100 MHz, DMSO-d_6) $\delta = 160.0$, 148.1, 146.0, 141.2, 134.7, 132.1, 131.6, 128.6, 127.0, 126.2, 123.1, 121.0, 120.4, 119.3; HRMS (ESI-TOF) *m/z*: $[M+Na]^+$ Calcd for $C_{19}H_{13}N_3O_4SNa$: 402.0518 $[M+Na]^+$; Found 402.0518.

4.4.12. N-(acridin-9(10H)-ylidene)-4-(trifluoromethyl) benzenesulfonamide (**3l**)

Yellowish solid (58 mg, 56%). mp: 230–232 °C; IR (KBr, cm^{-1}): 2924, 1633, 1061, 824: ^{1}H NMR (400 MHz, DMSO-d_6) $\delta = 13.08$ (br s, 1H), 8.68 (d, $J = 8.5$ Hz, 2H), 8.22 (d, $J = 8.0$ Hz, 2H), 8.00 (d, $J = 8.5$ Hz, 2H), 7.95–7.84 (m, 2H), 7.76 (d, $J = 8.3$ Hz, 2H), 7.44 (t, $J = 7.7$ Hz, 2H); ^{13}C NMR (100 MHz, DMSO-d_6) $\delta = 160.4$, 149.7, 140.5, 135.0, 131.8, 131.4, 128.8, 126.6 (q, 3JC-F = 3.7 Hz), 126.8, 123.1, 118.6, 118.4; HRMS (ESI-TOF) *m/z*: $[M+Na]^+$ Calcd for $C_{19}H_{13}N_3O_4SNa$: 425.0542 $[M+Na]^+$; found 425.05386.

4.4.13. N-(acridin-9(10H)-ylidene)naphthalene-1-sulfonamide (**3m**)

Yellow solid (49 mg, 55%). mp: 245–247 °C; IR (KBr, cm^{-1}); 3420, 2919, 1628, 1100, 801. ^{1}H NMR (400 MHz, DMSO-d_6) ^{1}H NMR

Please cite this article in press as: Chourasiya SS, et al., N-(acridin-9-yl)arenesulfonamides: Synthesis, quantum chemical studies and crystal structure analysis to establish the tautomeric preferences, Tetrahedron (2018), https://doi.org/10.1016/j.tet.2018.05.024

(400 MHz, DMSO-d_6) $\delta = 12.98$ (br s, 1H), 8.67 (d, $J = 8.3$ Hz, 1H), 8.61 (d, $J = 8.3$ Hz, 2H), 8.28 (d, $J = 7.8$ Hz, 1H), 8.22 (d, $J = 8.3$ Hz, 1H), 8.11 (d, $J = 8.3$ Hz, 1H), 7.85 (t, $J = 6.8$ Hz, 2H), 7.74 (d, $J = 8.5$ Hz, 2H), 7.70–7.60 (m, 3 H), 7.32 (t, $J = 7.4$ Hz, 2H); ^{13}C NMR (100 MHz, DMSO-d_6) $\delta = 159.8, 140.8, 140.5, 134.8, 134.4, 133.2, 129.2, 128.9, 128.2, 127.6, 127.0, 126.2, 125.8, 125.0, 122.8, 118.7, 118.3$. HRMS (ESI-TOF) *m/z*: $[M+Na]^+$ Calcd for $C_{23}H_{16}N_2NaO_2S$: 407.0824 $[M+Na]^+$; found 407.0823.

*4.4.14. N-(acridin-9(10H)-ylidene)naphthalene-2-sulfonamide (**3n**)*

Yellowish solid (49 mg, 57%). mp: 240–242 °C; IR (KBr, cm^{-1}): 3434, 2923, 1632, 1063, 745; ^{1}H NMR (400 MHz, DMSO-d_6) $\delta = 12.92$ (br s, 1H), 8.72 (d, $J = 8.5$ Hz, 2H), 8.58 (s, 1H), 8.23–8.12 (m, 2H), 8.06 (dd, $J = 4.1, 7.9$ Hz, 2H), 7.88 (t, $J = 7.7$ Hz, 2H), 7.74 (d, $J = 8.3$ Hz, 2H), 7.68 (t, $J = 7.8$ Hz, 2H), 7.41 (t, $J = 7.8$ Hz, 2H); ^{13}C NMR (100 MHz, DMSO-d_6) $\delta = 160.0, 143.1, 140.5, 134.8, 134.2, 132.3, 129.7, 129.5, 128.6, 128.2, 127.9, 127.8, 125.4, 123.0, 122.9, 118.7, 118.3$. HRMS (ESI-TOF) *m/z*: $[M+Na]^+$ Calcd for $C_{23}H_{16}N_2NaO_2S$: 407.0824 $[M+Na]^+$; Found 407.0823.

*4.4.15. N-(acridin-9(10H)-ylidene)quinoline-8-sulfonamide (**3o**)*

Brown solid (49 mg, 55%). mp: 250–252 °C; IR (KBr, cm^{-1}): 3408, 2960, 2921, 1662, 1096, 799; ^{1}H NMR (400 MHz, DMSO-d_6) $\delta = 12.76$ (br s, 1 H), 8.82 (d, $J = 1.7$ Hz, 1H), 8.53 (t, $J = 8$ Hz, 4H), 8.27 (d, $J = 8$ Hz, 1H), 7.79–7.84 (m, 3H), 7.70 (d, $J = 8$ Hz, 2H), 7.60–7.63 (m, 1 H); 7.26 (d, $J = 8$ Hz, 2H); ^{13}C NMR (100 MHz, DMSO-d_6) $\delta = 158.0, 151.1, 140.4, 137.0, 134.6, 133.2, 129.2, 125.8, 122.3, 118.9, 117.9$; HRMS (ESI-TOF) *m/z*: $[M+Na]^+$ Calcd for $C_{22}H_{15}N_3NaO_2S$: 408.0777 $[M+Na]^+$; Found 408.0775.

Acknowledgments

The authors thank the Department of Science and Technology (DST), New Delhi for financial support.

Appendix A. Supplementary data

Supplementary data related to this article can be found at https://doi.org/10.1016/j.tet.2018.05.024.

References

1. Costes N, Le Deit H, Michel S, et al. *J Med Chem*. 2000;43:2395.
2. Martins ET, Baruah H, Kramarczyk J, et al. *J Med Chem*. 2001;44:4492.
3. Ketron AC, Denny WA, Graves DE, Osheroff N. *Biochemistry*. 2012;51:1730.
4. Fernández-Álvaro E, Hong WD, Nixon GL, O'Neill PM, Calderón F. *J Med Chem*. 2016;59:5587.
5. Sasikala WD, Mukherjee A. *J Phys Chem B*. 2012;116:12208.
6. Ajeet A, Mishra AK, Kumar A. *Am J Pharmacol Sci*. 2015;3:18.
7. Sanphui P, Sarma B, Nangia A. *Cryst Growth Des*. 2010;10:4550.
8. Bag PP, Kothur RR, Malla Reddy C. *CrystEngComm*. 2014;16:4706.
9. Onda N, Tanaka Y, Hino M, Gemma A. *Res Med Case Rep*. 2015;14:19.
10. Dai T, Huang Y-Y, Sharma SK, Hashmi JT, Kurup DB, Hamblin MR. *Recent Pat Anti Infect Drug Discov*. 2010;5:124.
11. Fox CL, Modak SM. *Antimicrob Agents Chemother*. 1974;5:582.
12. Gopi SP, Ganguly S, Desiraju GR. *Mol Pharm*. 2016;13:3590.
13. Majewsky M, Wagner D, Delay M, Bräse S, Yargeau V, Horn H. *Chem Res Toxicol*. 2014;27:1821.
14. Maury L, Rambau J, Pauvert B, Lasserre Y, Berge G, Audran M. *J Pharmacol Sci*. 1985;74:422.
15. Fisherman JS, Osborn BL, Chun HG, et al. *Invest N Drugs*. 1993;11:1.
16. Gao H, Yamasaki EF, Chan KK, Shen LL, Snapka RM. *Cancer Res*. 2000;60:5937.
17. Murugesan N, Gu Z, Spergel S, et al. *J Med Chem*. 2003;46:125.
18. Weiss MM, Dineen TA, Marx IE, et al. *J Med Chem*. 2017;60:5990.
19. Swain NA, Batchelor D, Beaudoin S, et al. *J Med Chem*. 2017;60:7029.
20. Sleebs BE, Czabotar PE, Fairbrother WJ, et al. *J Med Chem*. 2011;54:1914–1926.
21. Milletti F, Vulpetti A. *J Chem Inf Model*. 2010;50:1062–1074.
22. Topiol S, Weinstein H, Osman RJ. *Med Chem*. 1984;27:1531–1533.
23. Bharatam PV, Patel DS, Iqbal PJ. *Med Chem*. 2005;48:7615–7622.
24. Di Martino RMC, De Simone A, Andrisano V, et al. *Med Chem*. 2016;59:531–544.
25. Milletti F, Storchi L, Sforna G, Cross S, Cruciani GJ. *Chem Inf Model*. 2009;49:68–75.
26. Guasch L, Peach ML, Nicklaus MC. *J Org Chem*. 2015;80:9900–9909.
27. Oellien F, Cramer J, Beyer C, Ihlenfeldt WD, Selzer PM. *J Chem Inf Model*. 2006;46:2342–2354.
28. Pospisil P, Ballmer P, Scapozza L, Folkers GJ. *Recept Signal Transduct*. 2003;23:361–371.
29. Wojnarowska Z, Paluch M. *Disord. Pharm. Mater.*. Wiley-VCH Verlag GmbH & Co. KGaA; 2016:183–200.
30. Katritzky AR, Hall CD, El-Gendy BEDM, Draghici BJ. *Comput Aided Mol Des*. 2010;24:475–484.
31. Derat E, Shaik S. *J Am Chem Soc*. 2006;128:8185–8198.
32. Li D, Fedeles BI, Singh V, et al. *Proc Natl Acad Sci*. 2014;111:E3252–E3259.
33. Sakashita R, Oka Y, Akimaru H, et al. *Org Chem*. 2017;82:8686–8696.
34. Glaser R, Murmann RK, Barnes CLJ. *Org Chem*. 1996;61:1047–1058.
35. Long S, Zhang M, Zhou P, Yu F, Parkin S, Li T. *Cryst Growth Des*. 2016;16:2573–2580.
36. Chourasiya SS, Kathuria D, Nikam SS, et al. *J Org Chem*. 2016;81:7574–7583.
37. Ramakrishnan A, Chourasiya SS, Bharatam PV. *RSC Adv*. 2015;5:55938–55947.
38. Chourasiya SS, Kathuria D, Singh S, Sonwane VC, Chakraborti AK, Bharatam PV. *RSC Adv*. 2015;5:80027–80038.
39. Lammertsma K, Prasad BV. *J Am Chem Soc*. 1994;116:642–650.
40. Chourasiya SS, Patel DR, Nagaraja CM, Chakraborti AK, Bharatam PV. *New J Chem*. 2017;41:8118–8129.
41. The *N*-(acridin-9-yl)-benzenesulfonamide represents the only literature report of this class (NAAS) of compounds Gurewitsch S. *Zh Fiz Khim*. 1962;36:734–741.
42. Bahrami K, Khodaei MM, Soheilizad MJ. *Org Chem*. 2009;74:9287–9291.
43. Luci DK, Jameson JB, Yasgar A, et al. *J Med Chem*. 2014;57:495–506.
44. Surman MD, Mulvihill MJ, Miller MJ. *Org Lett*. 2002;4:139–141.
45. Hu W, Guo Z, Chu F, et al. *Med Chem*. 2003;11:1153–1160.
46. Jafarpour M, Rezaeifard A, Aliabadi M. *Appl Catal A*. 2009;358:49–53.
47. Mohamed SF, Kotb ER, Abd El-Meguid EA, Awad HM. *Res Chem Intermed*. 2017;43:437–456.
48. Deng X, Mani NS. *Green Chem*. 2006;8:835–838.
49. Baffoe J, Hoe MY, Touré BB. *Org Lett*. 2010;12:1532–1535.
50. Han X. *Tetrahedron Lett*. 2010;51:360–362.
51. Wang X, Guram A, Ronk M, Milne JE, Tedrow JS, Faul MM. *Tetrahedron Lett*. 2012;53:7–10.
52. Burton G, Cao P, Li G, Rivero R. *Org Lett*. 2003;5:4373–4376.
53. Jiang Y, You Y, Dong W, Peng Z, Zhang Y, An DJ. *Org Chem*. 2017;82:5810–5818.
54. Allen CFH, McKee GHW. *Acridone. In Org. Synth*. John Wiley & Sons, Inc; 2003.
55. Allen C. *Org Synth*. 1939;19:6–9.
56. Barfield M, Fagerness P. *J Am Chem Soc*. 1997;119:8699–8711.
57. Parr RG, Yang W. *Density-functional Theory of Atoms and Molecules*. New York: Oxford University Press; 1989.
58. Schleyer PVR, Maerker C, Dransfeld A, Jiao H, Hommes NJR vE. *J Am Chem Soc*. 1996;118:6317–6318.
59. Stanger A. *J Org Chem*. 2006;71:883–893.
60. Fallah-Bagher-Shaidaei H, Wannere CS, Corminboeuf C, Schleyer PvR. *Org Lett*. 2006;8:863.
61. Parker AJ. *Chem Rev*. 1969;69:1.
62. Wyman J. *J Am Chem Soc*. 1933;55:4116.
63. Chakraborti AK, Sharma R, Nayak MK. *J Org Chem*. 2002;67:6406.
64. Chakraborti AK, Sharma R, Nayak MK. *J Org Chem*. 2002;67:2541.
65. Kuz´mina LG, Struchkov YT. *Cryst Struct Commun*. 1981;10:25.
66. Crystal data for 3n: $C_{23}H_{16}N_2O_2S$, M = 384.45, Triclinic, space group Pī, a = 9.9645(10) Å, b = 16.8999(18) Å, c = 18.3161(18) Å, α = 65 °, β = 79°, γ = 82°, V = 2726(5)Å^3, Z = 6, D_c = 1.405 g/cm^3, μ(Mo-Kα) = 0.200 mm^{-1}, T = 298(2) K, 13549 reflections collected. Refinement of 8500 reflections with I>2σ(I) converged at a final R1 = 0.056, wR2 = 0.1376, gof = 1.020.
67. Reimers JR, Cai Z-L, Bilic A, Hush NS, Ann NY. *Acad Sci*. 2003;1006:235.
68. Liu X, Subotnik J. *J Chem Theor Comput*. 2014;10:1004–1020.
69. Chai JD, Head-Gordon M. *Phys Chem Chem Phys*. 2008;10:6615.
70. Frisch MJ, Trucks GW, Schlegel HB, et al. *Gaussian*. Wallingford CT: Inc.; 2009.
Lee C, Yang W, Parr, RG. Phys Rev B, 1988;37:785.
71. Lee C, Yang W, Parr RG. *Phys Rev B*. 1988;785:789.
72. Cancès E, Mennucci B, Tomasi J. *J Chem Phys*. 1997;107:3032.
73. Reed AE, Weinstock RB, Weinhold F. *J Chem Phys*. 1985:83.